JOURNAL OF SOLID STATE CHEMISTRY 108, 260–266 (1994)

Structural Study of the Solid Solutions in a $CaSi_2$–$LaSi_2$ System

Hideyuki Nakano and Shoji Yamanaka

Department of Applied Chemistry, Faculty of Engineering, Hiroshima University, Higashi-Hiroshima 724, Japan

Received January 29, 1993; in revised form May 25, 1993; accepted May 27, 1993

The crystal structure of the solid solutions in a $CaSi_2$–$LaSi_2$ system was studied by the X-ray Rietveld analysis. The layered structure of $CaSi_2$ was changed into the three-dimensional α-$ThSi_2$-type structure in the solid solutions $Ca_{1-x}La_xSi_2$ ($0.2 \leq x \leq 1.0$). The lattice parameters of the solid solutions did not obey Vegard's rule. The structural analysis revealed that the Si–Si distances and the Si(–Si)–Si bond angle of the three-coordinated coplanar group of the Si sublattice changed rather irregularly with the composition of the solid solutions. The Raman band due to the Si–Si stretching vibration was hardly influenced by the composition of the solid solutions. Magnetic susceptibility measurements suggested that the superconducting transition of the solid solution occurred at a temperature between 1.5 and 2.5 K.

INTRODUCTION

Calcium disilicide $CaSi_2$ is a Zintl phase with a formal charge of $Ca^{2+}(Si^-)_2$, where the silicide anion is isoelectronic with group V elements and forms an anion sublattice with a corrugated layer structure like As (1). The calcium ions are sandwiched between the corrugated silicon layers (Fig. 1a) (2). Among a number of disilicides of alkaline-earth and rare-earth metals, this type of layered structure is very special. Most of the disilicides adopt the α-$ThSi_2$ structure, in which planar three-coordinated silicon groups are connected with each other by twisting alternatively by 90° so as to form a tetragonal three-dimensional open network (3); the metal atoms are placed in the interstices and bonded to 12 Si neighbors (Fig. 1b). If the layered structured $CaSi_2$ is compressed under a high pressure and high temperature, it is transformed into the α-$ThSi_2$ structure (4).

Strontium disilicide, $SrSi_2$ with metal atoms larger than Ca cannot have a layered structure, but rather have a cubic three-dimensional network (5). Although the structure of $SrSi_2$ also consists of planar three-bonded silicon groups, the way the groups are connected is very different from the way they are connected in the α-$ThSi_2$ structure. $SrSi_2$ can be transformed to the α-$ThSi_2$ structure by a high pressure and high temperature treatment (4). In the structure of $BaSi_2$ which has much larger metal atoms, the silicon atoms exist as Si_4 clusters isolated by Ba atoms (5). $BaSi_2$ is transformed to the $EuGe_2$ structures by treatment under a high pressure and high temperature (6). The $EuGe_2$ structure includes a trigonal layered silicon sublattice like the corrugated silicon layers in the $CaSi_2$ structure.

Evers *et al.* (7) studied three kinds of solid solution systems $M_{1-x}M'_xSi_2$ (M, M' = Ca, Sr, Eu). The metallic radii (8) of these metals for coordination number 12 are 1.974 Å (Ca), 2.050 Å (Eu), and 2.148 Å (Sr). $EuSi_2$ was considered to be the most stable α-$ThSi_2$ structure, for the same structure was obtained in not only high but also normal pressure syntheses. The substitution of the Ca atoms with larger Eu atoms stabilized the α-$ThSi_2$ structure over a pretty wide range of $0.2 \leq x \leq 1.0$ in the system $Ca_{1-x}Eu_xSi_2$ even in normal pressure synthesis. Similarly, the substitution of the Sr atoms with smaller Eu atoms also extends the formation region of the α-$ThSi_2$ structure to the range $0.2 \leq x \leq 1.0$ in the system $Sr_{1-x}Eu_xSi_2$. The solid solutions with the α-$ThSi_2$ structure in the system $Ca_{1-x}Sr_xSi_2$ were prepared only in a high-pressure synthesis. The lattice parameters of these solid solutions with the α-$ThSi_2$-type structure obeyed Vegard's rule. Evers *et al.* (9) extended their studies to the solid solutions with $BaSi_2$ having much larger metal atoms, and arrived at the conclusion that the structure type of disilicides was mainly determined by size relations of the metal atoms to the silicon sublattice.

In the present paper, a new solution series of $CaSi_2$–$LaSi_2$ has been studied, where Ca atoms are substituted with La atoms. $LaSi_2$ has a homogeneity range from $LaSi_2$ to $LaSi_{1.83}$, accompanied by a change of structure from the α-$ThSi_2$ to the $GdSi_2$ type (10). The trivalent metallic radius of La for coordination number 12 is 1.804 Å, which is smaller than Ca (1.974 Å) and much smaller than Eu (2.084 Å). The solid solutions with the α-$ThSi_2$ structure have been obtained over a wide range of compo-

0022-4596/94 $6.00

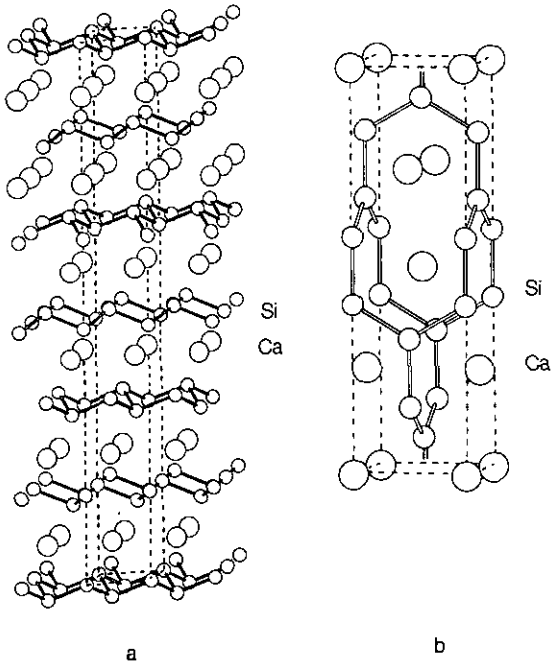

FIG. 1. Schematic structural model of $CaSi_2$; (a) layer–structured 6R type and (b) high-pressure form of the α-$ThSi_2$ type.

sitions. The structures of a series of the solid solutions are investigated by the X-ray powder Rietveld analysis, and some physical properties of the solid solutions are studied.

EXPERIMENTAL

Preparation of Solid Solutions

$CaSi_2$ was prepared by melting a constituent mixture of Ca metal which was purified by sublimation under a vacuum at 900°C, and Si (99.99%) in a water-cooled copper crucible with RF induction heating under an Ar atmosphere. The apparatus and the detailed procedures were described elsewhere (11). $LaSi_2$ was prepared in a similar manner by using La metal of reagent grade (99.9%) from Mitsuwa Chemicals and the Si used in the preparation of $CaSi_2$. The two kinds of silicides prepared were mixed in different ratios and melted in the same water-cooled copper crucible under an Ar atmosphere. The melts were cooled down to room temperature in the crucible by decreasing the RF power.

Analyses

X-ray powder diffraction (XRD) patterns were measured by using graphite monochromatized CuKα radiation with Si powder as an internal standard. The structures of the solid solutions were analyzed on the basis of the XRD patterns by using a RIETAN X-ray powder Rietveld analysis program contained in the X-ray diffractometer (Rigaku, model RAD-R). Raman spectroscopic measurements were made on a Raman spectrometer (Japan Spectroscopic Co., model NR-1800) with radiation of 514.5 nm of an Ar^+ ion laser with a power of 100 mW. Magnetic susceptibility measurements were

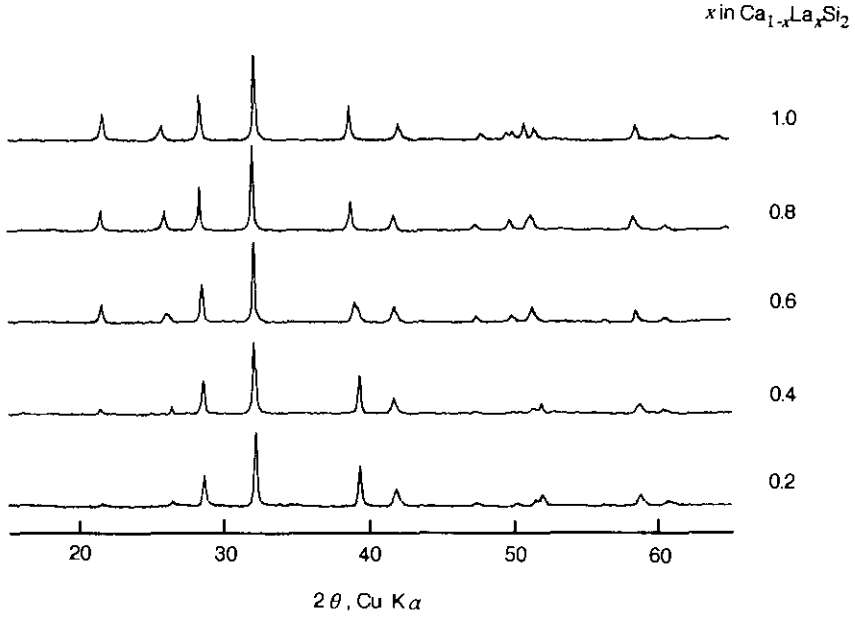

FIG. 2. X-ray powder diffraction patterns of a series of solid solutions $Ca_{1-x}La_xSi_2$.

performed in the temperature range 2–25 K using a SQUID magnetometer.

RESULTS AND DISCUSSION

XRD Study

The XRD patterns of the solid solutions $Ca_{1-x}La_xSi_2$ prepared are shown in Fig. 2. As seen from the figure, the intensities and diffraction angles of the peaks are systematically changed or shifted with respect to those of $LaSi_2$ of the α-$ThSi_2$ structure. This finding suggests that the ternary silicide system adopts the α-$ThSi_2$ structure and that the Ca and La atoms are randomly mixed at the metal sites. If the amount of the substitution of Ca with La is 0.1 in x, a mixture of layer-structured $CaSi_2$ and a phase of the α-$ThSi_2$ type is obtained. The lowest solubility limit for the α-$ThSi_2$ structure was estimated to be about 0.2 in x.

All the diffraction peaks of each XRD pattern could be indexed on the basis of a tetragonal unit cell for the α-$ThSi_2$ structure. The lattice parameters calculated by the least-squares method are shown as a function of the composition (x) in Fig. 3. It should be noted that the a and the c parameters do not hold to Vegard's rule at all, although the cell volume increases almost linearly with the increase of the content of $LaSi_2$. This result is in strong contrast to the fact that the lattice parameters of the solid solutions in the systems $M_xM'_{1-x}Si_2$ (M, M' = Ca, Sr, Eu) changed linearly with the composition (7). It is shown in Fig. 2 that the XRD pattern of the corresponding sample ($x = 0.6$) has broadened reflections for (004) and (105) at 26° and 39°, respectively. These findings can be interpreted in terms of a presence of two phases with slightly different lattice parameters. The lattice parameters plotted for the sample with $x = 0.6$ can be regarded as the mean values of the two phases.

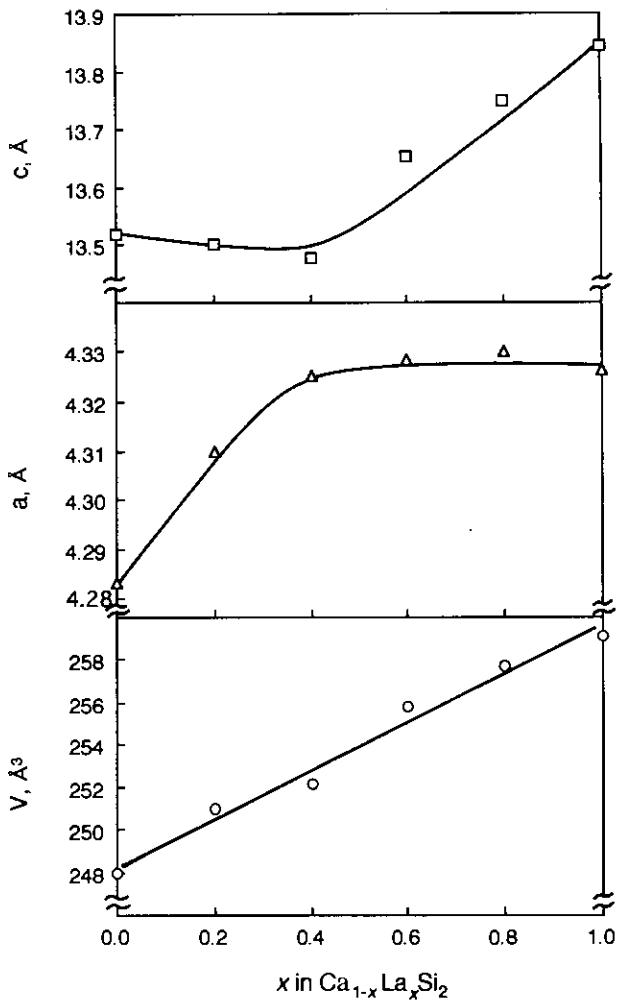

FIG. 3. Lattice parameters of the tetragonal unit cell as a function of x in the solid solutions $Ca_{1-x}La_xSi_2$. The parameters at $x = 0$ are of the high-pressure form of $CaSi_2$ reported by Evers *et al.* (12).

Structural Analysis

In order to investigate the origin of the unusual changes of the lattice parameters shown in Fig. 3, systematic structural analyses of a series of the solid solutions were performed by the X-ray Rietveld method. The analyses were carried out with 4500 data points over the diffraction angles between 15 and 65° on a space group $I4_1/amd$ of the α-$ThSi_2$ structure. The initial coordinates used for the positions of Si and metal atoms were those of $CaSi_2$ of the high-pressure form reported by Evers *et al.* (12), and no ordering of Ca and La atoms was assumed. One of the analytical results is given in Fig. 4, showing the observed and the calculated XRD patterns and the difference curve for the case of a solid solution of $Ca_{0.2}La_{0.8}Si_2$. The crystallographic data obtained by the Rietveld analyses are summarized in Table 1. On the basis of the data given in Table 1, two kinds of Si–Si bond lengths (1 and 2) and the bond angle (ϕ) of the coplanar three-bonded silicon group were calculated, which are shown in Fig. 5. The coplanar silicon triangle is illustrated as an inset of the figure with the indication of the two kinds of silicon bonds and the bond angle.

The silicon coplanar groups are not equilateral triangles, but are distorted to isosceles triangles. The initial increase of the a lattice parameter with the increase of the substitution amount of Ca with La (Fig. 3) can be attributed mainly to the increase of the bond angle ϕ. During this increase in a, the lattice parameter c is kept almost constant, because the increase in the Si–Si (1) bond length along the c axis is canceled by the depletion of the central Si atom caused by the increase in the bond angle ϕ. In the solid solutions $Ca_{1-x}La_xSi_2$ of a range $0.6 \leq x \leq 1.0$, the reversed situation is true; the increase in the c parameter is caused by the sharpening of the bond

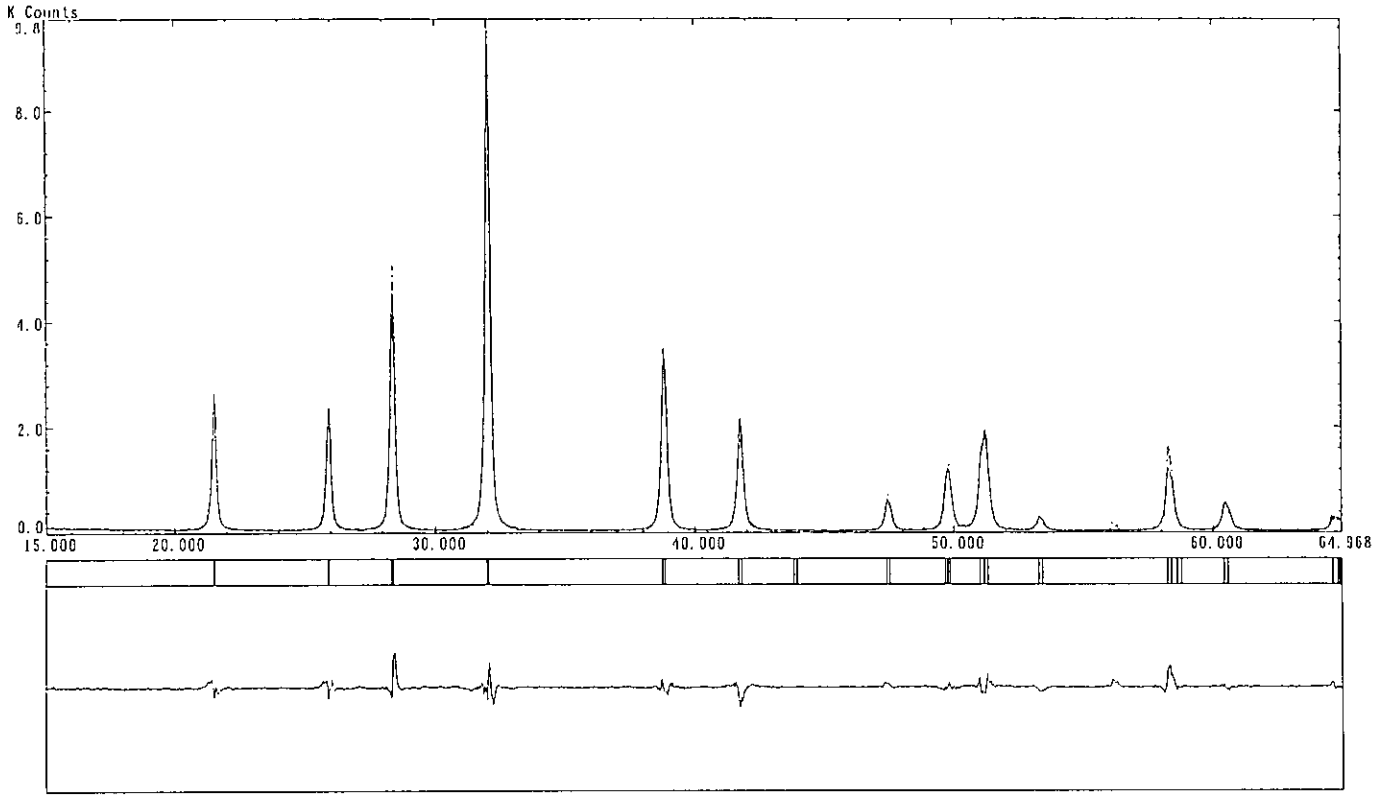

FIG. 4. Typical Rietveld analysis result for a sample $Ca_{0.2}La_{0.8}Si_2$ showing the observed (points) and calculated (solid line) profiles with the difference curve (bottom).

angle ϕ, coupled with the increase in the bond length of the Si–Si (2) bond, while the "a" parameter remains almost constant.

Raman Spectra

The Raman spectra of the solid solutions of this region were measured and are compared with that of layer-structured $CaSi_2$ in Fig. 6. The silicides have an intense Raman band at about 510 cm^{-1}, which is comparable to the frequency of the band due to the Si–Si stretching vibration of elemental silicon (516–520 cm^{-1}) (13). The Raman band of the solid solutions and $LaSi_2$ is shifted only slightly toward a lower frequency with respect to that of the layer-structured $CaSi_2$, but the shift of the frequency is hardly influenced by the composition of the solid solutions. This

TABLE 1
Crystallographic Data for the Solid Solutions Obtained by the Rietveld Analysis

	Composition, x in $Ca_{1-x}La_xSi_2$					
	0[a]	0.2	0.4	0.6	0.8	1
Lattice parameter						
a (Å)	4.283(3)	4.310(6)	4.325(5)	4.329(1)	4.330(1)	4.326(1)
c (Å)	13.53(1)	13.50(2)	13.47(2)	13.65(4)	13.75(1)	13.84(1)
Atomic position						
Si (8*e*); 0, 0, z	0.41505(5)	0.414(3)	0.413(2)	0.414(4)	0.414(2)	0.416(3)
Ca, La (4*a*); 0, 0, 0						
Reliability factors (%)						
R_{wp}		21.99	18.30	21.59	13.88	18.47
R_I		7.47	5.85	6.91	3.39	6.03

[a] The data for the high-pressure form of $CaSi_2$ were taken from Ref. (*12*).

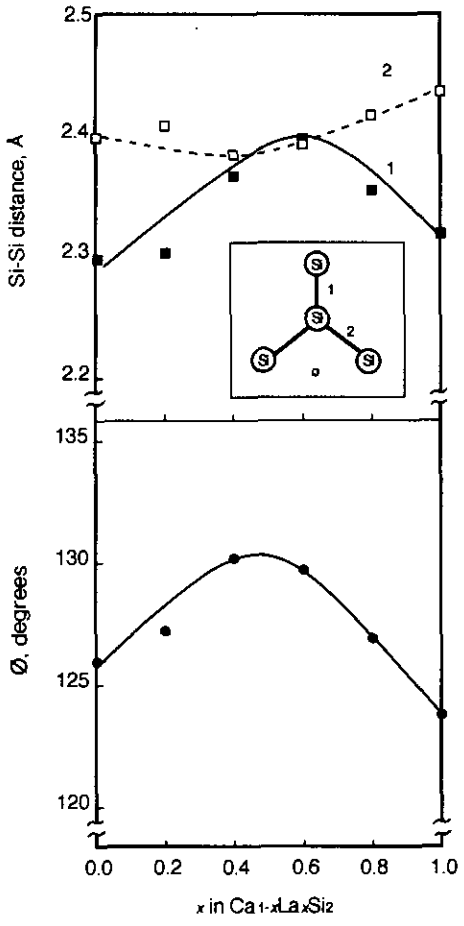

FIG. 5. The Si–Si bond lengths and the bond angle of the coplanar three-bonded silicon group as a function of the composition. A silicon triangle is shown in the inset.

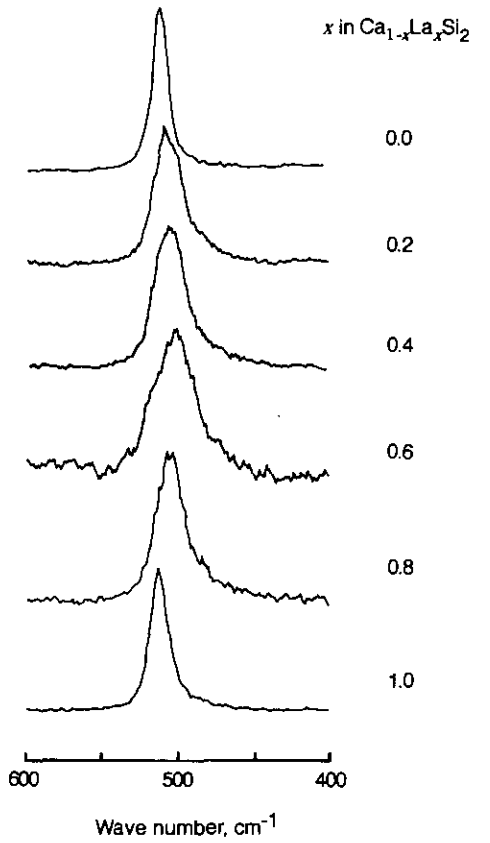

FIG. 6. Raman spectra of the Si–Si stretching vibration region of a series of solid solutions $Ca_{1-x}La_xSi_2$ with the α-$ThSi_2$ structure. The spectrum of the layer-structured $CaSi_2$ ($x = 0$) is shown for comparison.

finding suggests that the Si–Si vibrational frequency is determined mainly by the structural type of the silicon sublattice.

Magnetic Susceptibility

The high-pressure forms of $CaSi_2$ and $LaSi_2$ are superconductors with transition temperatures (T_c) at 1.58 (14) and 2.5 *K* (15), respectively. Magnetic susceptibilities of the solid solutions were measured to see if the superconducting transition occurred in a similar temperature range. The magnetic susceptibility of a solid solution $Ca_{0.3}La_{0.7}Si_2$ is shown in Fig. 7; a diamagnetic decrease in the susceptibility is observed at 2.5 K in the curve, which can be attributed to the superconducting transition. Due to the limitation of the temperature control of the magnetometer used, the transitions which would occur below 2 K could not be measured. However, it would be very likely that all the solid solutions have T_c between 1.58 and 2.5 K.

Structural Consideration

The metallic radius of alkali-earth and rare-earth metals for coordination number 12 is plotted in Fig. 8 as a function of the cubic root of the cell volume for a unit formula (MSi_2) (5, 16–19), $\sqrt[3]{V/n}$, of the corresponding metal disilicide; the structural types of the metal disilicides are distinguished by different markers in the figure. It should be noted that the formation region of a specific structure is lined by the cell volume of the disilicides rather than by the size of the metallic radius. The α-$ThSi_2$ structure is adopted by a large number of metal disilicides with $\sqrt[3]{V/n}$ in the range 4.03–3.72 Å. The cell volumes of $CaSi_2$ and $SrSi_2$ can be compressed into this region by a high-pressure treatment, and these crystals are transformed to the α-$ThSi_2$ structure (4). The cell volume of $BaSi_2$ is too large to be compressed to the α-$ThSi_2$ region even under high pressure. It is transformed to the $EuGe_2$ structure, a trigonal-layered structure different from the $CaSi_2$-type layer structure. The late 4*f* rare-earth metal disilicides have the AlB_2 structure, in which the silicon atoms are arranged in coplanar hexagonal net-like graphite and the metal atom layer is sandwiched between the

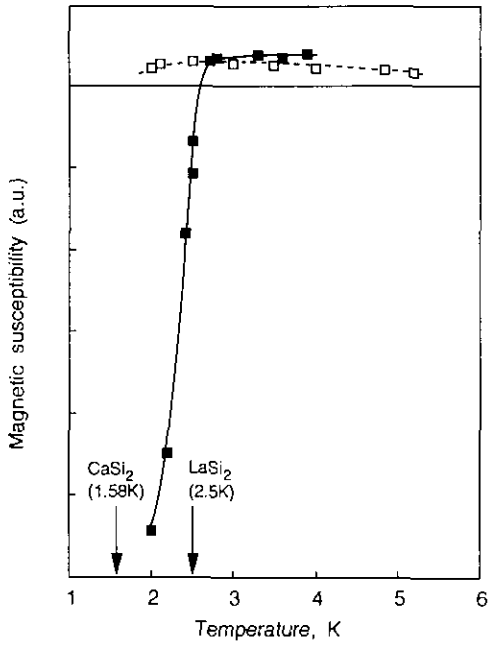

FIG. 7. Magnetic susceptibility of solid solutions as a function of temperature; (■) $Ca_{0.3}La_{0.7}Si_2$ and (□) $Ca_{0.7}La_{0.3}Si_2$. The superconducting transition temperatures reported for the high-pressure form of $CaSi_2$ and $LaSi_2$ are indicated by arrows.

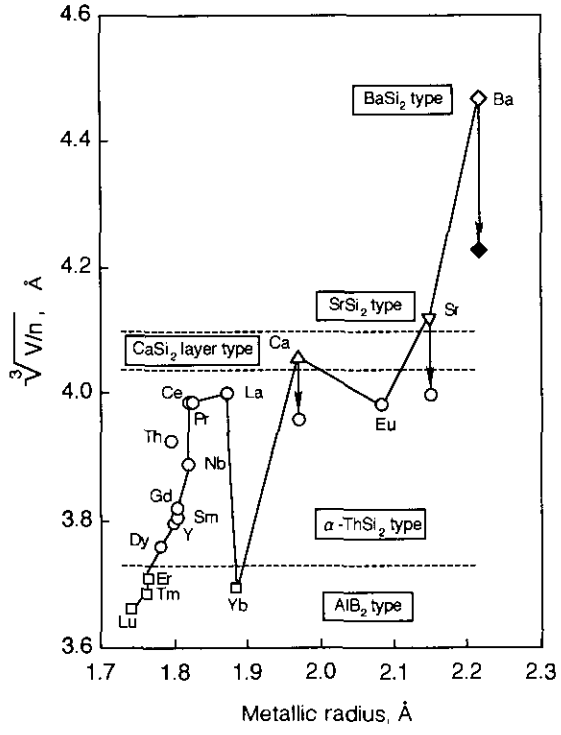

FIG. 8. Formation regions of various types of metal disilicides in a plot of $\sqrt[3]{V/n}$ (the cubic root of the cell volume per unit formula MSi_2) vs the metallic radii for 12 coordination. The data for the cell volumes are taken from Refs. (5) (M = Ba, Sr, Ca), (16) (M = La, Pr, Ce, Nb, Sm), (17) (M = Gd, Y, Dy), (18) (M = Er, Tm, Lu, Yb), and (19) ($ThSi_2$). The structural types are distinguished by different markers; (◇) $BaSi_2$, (▽) $SrSi_2$, (△) $CaSi_2$, (◆) $EuGe_2$, (○)α-$ThSi_2$, and (□) AlB_2, $BaSi_2$, $SrSi_2$ and $CaSi_2$ are converted into the corresponding high-pressure forms.

silicide layers (20). Actually, these are defect "disilicides" with the composition RSi_{2-x} (21). The metal "disilicides" with the AlB_2 layer structure have the smallest cell volumes. It is interesting to note that $EuSi_2$ has the α-$ThSi_2$ structure irrespective of its large metallic radius. Probably the metallic radius of Eu may be overestimated in this structure. As the metallic radius of La is originally much smaller than that of Eu, the substitution of Ca with La would be more favorable for the stabilization of the α-$ThSi_2$ structure.

Recently, the chemical and electronic structures of calcium silicides have been extensively studied (22–24), since the understanding of the interaction of Ca with Si surface is very important in the microelectronics industries. The theoretical and electron photoemission studies of $CaSi_2$ suggested that the chemical interaction between the silicon and calcium cannot be interpreted in terms of only ionic character, although there is a large difference between the electronegativities of the two elements. A covalent character is present together with some ionic contribution. A series of RPtSi phases with ordered α-$ThSi_2$ structure was prepared by Klepp and Parthé (25), where R = La, Ce, Pr, Nd, Sm, and Gd. All these early 4f rare-earth elements have α-$ThSi_2$ structure, half of the Si sites of α-$ThSi_2$ being substituted with Pt in an ordered manner. They found that the cubic root of the cell volume decreases linearly with the decrease of the R^{3+} cation radius. The late rare-earth metal series from R = Tb to Lu has the AlB_2-type structure with a little drop of the cell volume (cubic root) with the cation radius. Their finding on a relationship between the cationic radii of the metals and the cell volumes suggests that the idea of cationic contribution would be still important.

A remarkable deviation from Vegard's rule was found in a system $Ca_{1-x}La_xSi_2$ (Fig. 3). This finding was interpreted in terms of a nonuniform structural change of the coplanar three-bonded silicon groups (Fig. 5). The metallic radius of La may vary with the composition between divalent (1.924 Å) and trivalent (1.871 Å) metallic radii. It is also very likely that the degree of the covalent contribution is variable with the composition. These effects are mixed together and may give rise to a nonuniform structural change of the three-bonded silicon group. For more detailed discussion, systematic studies of other solid solution systems are necessary, and structural data by a single crystal analysis would be preferred to the Rietveld powder analysis.

ACKNOWLEDGMENTS

This study was partly defrayed by the Grant-in-Aid for Scientific Research on Priority Area of the Ministry of Education, Science and Culture. The authors acknowledge Professors T. Fujita and Y. Maeno of the Faculty of Science, Hiroshima University for the use of the SQUID magnetometer and discussions.

REFERENCES

1. H. Schäfer, B. Eisenmann, and W. Muller, *Angew. Chem. Inter. Edit. Engl.* **12,** 694 (1973).
2. J. Böhm and O. Hassel, *Z. Anorg. Allg. Chem.* **160,** 152 (1927).
3. A. F. Wells, "Structural Inorganic Chemistry," 5th ed., p. 991. Clarendon, Oxford, 1984.
4. J. Evers, *J. Solid State Chem.* **20,** 173 (1977).
5. K. H. Janzon, H. Schäfer, and A. Weiss, *Z. Anorg. Allg. Chem.* **372,** 87 (1979).
6. J. Evers, *J. Solid State Chem.* **32,** 77 (1980).
7. J. Evers, G. Oehlinger, and A. Weiss, *J. Less-Common Met.* **60,** 249 (1978).
8. L. Pauling, "The Nature of The Chemical Bond," 3rd ed., Chap. 3. Cornell Univ. Press, New York, 1960.
9. J. Evers, G. Oehlinger, and A. Weiss, *J. Less-Common Met.* **69,** 399 (1980).
10. E. I. Gladyshevsky, "Crystal Chemistry of Silicides and Germanides, Metallurgyia." Moscow (1971).
11. S. Yamanaka, H. Itho, and M. Hattori, *in* "Zeolite and Pillared Clay Synthesis" (M. L. Occelli and H. Robson, Eds.), p. 296. Van Nostrand–Reinhold, Princeton, New Jersey, 1992.
12. J. Evers, G. Oehlinger, and A. Weiss, *Z. Naturforsch. B* **37,** 1487 (1982).
13. W. N. Hansen, *J. Opt. Soc. Am.* **58,** 380 (1968).
14. G. F. Hardy and J. K. Huml, *Phys. Rev.* **93,** 1004 (1954).
15. W. E. Henry, C. Betz, and H. Muir, *Bull. Am. Phys. Soc.* **7,** 474 (1962).
16. G. Brauer and H. Haag, *Z. Anorg. Allg. Chem.* **267,** 198 (1952).
17. J. A. Perri, E. Banks, and B. Post, *J. Phys. Chem.* **63,** 2073 (1959).
18. A. G. Tharp, *J. Phys. Chem.* **66,** 758 (1962).
19. P. Lejay, B. Chevalier, J. Etourneau, J. M. Tarascon, and P. Hagenmuller, *Mater. Res. Bull.* **18,** 67 (1983).
20. A. F. Wells, "Structural Inorganic Chemistry," 5th ed., p. 1053. Clarendon, Oxford, 1984.
21. A. Iandell, A. Palenzona, and G. L. Olcese, *J. Less-Common Metals* **64,** 213 (1979).
22. D. D. Sarma, W. Speier, L. Kumar, C. Carbone, A. Spinsanti, O. Bisi, A. Iandelli, G. L. Olcese, and A. Palenzona, *Z. Phys. B* **71,** 69 (1988).
23. P. Blaha and J. Callaway, *Phys. Rev. B* **32,** 7664 (1985).
24. A. Franciosi, J. H. Weaver and D. T. Peterson, *Phys. Rev. B* **31,** 3606 (1985).
25. K. Klepp and E. Parthë, *Acta Crystallogr., Sect. B* **38,** 1105 (1982).